

Of rats and rocks: using pre-clinical PET imaging facilities in core analysis

Bergit Brattækås^{1*}, Martin A. Fernø¹, Malin Haugen¹, Tore Føyen¹, Marianne Steinsbø¹, Arne Graue¹, Njål Brekke², Tom Christian Holm Adamsen², Cecilie Brekke Rygh³ and Heidi Espedal⁴

¹Dept. of Physics and Technology, University of Bergen, Norway

²Center for Nuclear Medicine - PET, Department of Radiology, Haukeland University Hospital, Norway

³Department of Radiology, Haukeland University Hospital, Norway

⁴Molecular Imaging Center, Department of Biomedicine, University of Bergen, Norway

Abstract. Positron emission tomography (PET) is routinely used for medical imaging; a current surge in published geoscientific research utilizing this modality also infer increasing interest for *in-situ* PET imaging in core analysis. Excellent signal to noise ratio coupled with high temporal and spatial resolution suggest that PET might become the new method-of-choice for core analysis. Obstacles related to production, transfer and handling of radioactive fluids and gases must, however, be dealt with for PET to become a widely used core scale imaging technique. This paper describes an ongoing, true multidisciplinary collaboration, where pre-clinical PET imaging facilities are routinely used in core analysis to investigate dynamic fluid flow at high pressure conditions. We detail challenges and opportunities related to porous media research in established pre-clinical laboratory facilities designed for small-animal imaging, and demonstrate the significant potential of PET imaging in core scale analysis in a context related to long-term porous media carbon storage.

Explicit imaging of several fluid phases is possible by PET imaging using a range of readily available radiotracers. Relevant radiotracers to carbon storage in porous media are e.g. the carbon radioisotope ¹¹C and water-soluble tracer ¹⁸F. These are both short-lived tracers (20 - 110 min) and must be used in high doses of radiation, which present challenges related to safe transfer and handling. Although there are several obstacles to conduct advanced core analysis in hospital imaging facilities (some of which are detailed in this paper), significant advantages include trained personnel on-site to operate a local cyclotron, procedures in place to ensure safe and efficient transfer of short-lived radiopharmaceuticals from the cyclotron, and advanced image analysis capabilities available. Cyclotrons are widely available worldwide (currently more than 1200 operating cyclotrons), often located in close proximity to medical and pre-clinical imaging facilities and academic institutions. Similar collaborations may therefore also be possible elsewhere, reducing the need for allocated geophysical PET-scanners and lowering the threshold for routinely using PET imaging in core analysis.

1 Background

1.1 A quick introduction to Positron Emission Tomography imaging

Positron emission tomography (PET) imaging utilizes positron-emitting radionuclides to gain insight into fluid flow and accumulation. These radionuclides are rich in protons and decay by beta plus decay; the spontaneous physical phenomenon where an emitted positron annihilates with an electron and consequently emits a pair of specific energy photons (511 keV) in opposite directions. PET scanners can determine annihilation

events with high spatial and temporal accuracy; by detecting gamma rays (photons) occurring simultaneously on opposite sides of an object. The number, position and size of PET detector elements, as well as the distance between the object and detectors, strongly influence the spatial resolution of PET imaging [1]. PET is established as a diagnostic tool in medicine, where the radioactively labelled “object” is often a human (in clinical imaging) or animal (in pre-clinical research) but has also recently been demonstrated as a highly useful tool for non-medical purposes: flow visualization in porous rocks [2-15]. For practical purposes the beta plus decay is insensitive to pressure and temperature [16]. PET imaging is, hence, a suitable tool to visualize fluid flow and accumulation

* Corresponding author: bergit.brattækås@uib.no

within core plugs placed in confinement vessels under high pressure and temperature conditions; e.g. to investigate porous media CO₂ storage at relevant storage conditions.

PET imaging has several advantages, which in sum renders PET a strong competitor to other imaging methods initially used for diagnostic purposes, e.g. computed tomography (CT) and magnetic resonance imaging (MRI). Advantages include 1) high spatial resolutions, 2) high temporal resolutions (i.e. possibility to investigate fast processes at high flow rates), 3) excellent signal-to-noise ratio (i.e. a small amount of radioactivity is sufficient to produce high-quality images; without altering the properties of the labelled fluid), 4) explicit detection of radioactively labelled fluid only (i.e. fluid flow paths are imaged without the porous medium influencing image quality). For a general introduction to PET imaging in water resources research we recommend Zahasky and Benson (2019) [21].

During core scale imaging by CT and MRI, high spatial resolution may be achieved by decreasing temporal resolution: a trade-off which must be set within each experiment. Micro-CT for example enables micrometer visualization of the pore space, but the time scale for acquiring 3D images is several hours. PET imaging does not suffer from this tradeoff: photon emissions are continuously recorded during imaging, and spatial and temporal resolutions are set during post-processing. 3D images may, hence, be achieved during short time spans (seconds), while maintaining a high spatial resolution. A simple schematic of imaging methods and resolution relations is shown in **Fig. 1**.

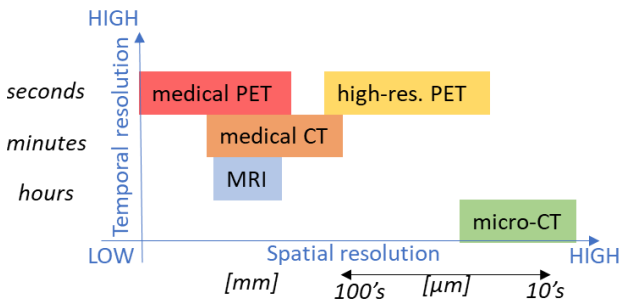


Fig 1. Imaging technologies used for 3D *in-situ* visualization of core material and core floods. Spatial resolution may be high for MRI and CT imaging, although that typically increases the scan time. PET images are post-processed; and maintain high spatial resolution regardless of temporal resolution preferences.

1.2 Existing opportunities

Although some research groups have procured or built their own PET imaging systems (e.g. [17-20]), this is not a realistic solution for the average core analyst. Several necessary specifications and requirements must be fulfilled and a number of challenges (both perceived and real, recently described by Zahasky *et al.* [21]) dealt with to perform core analysis with PET imaging. Most obstacles relate to the production, transportation, safe use and handling of radioisotopes, especially short-lived

radioisotopes, that are often used for geoscientific purposes. These obstacles are manageable, but requires significant funds and space for necessary equipment and personnel. The threshold for PET-imaging utilizing private facilities therefore remains high, and other options may be explored to make PET-imaging available for a broader range of users.

Hospitals world-wide are actively applying PET imaging for diagnostic purposes [22, 23], and clinical PET-scanners have become widespread during the last few decades. Obstacles related to production, transportation and safe handling of radioisotopes have therefore already been handled to routinely perform PET-imaging in hospitals. Clinical scanners are intended for human use, and are normally reserved for patients during operating hours. The time frame available for non-essential flow experiments is therefore limited. Access to operational IT infrastructure connected to clinical scanners is also restricted, to prevent insight into sensitive patient information. Further limitations related to cleanliness (operating potentially messy equipment in a sterile lab) and spatial resolution (limited to 2-5mm, because gantry and detector element sizes are constructed for human use [24]) in sum prevents clinical PET-scanners to be widely utilized in core analysis, although occasional experiments are feasible, and have been reported [2, 25, 26].

Another option also exists within many hospital research facilities: high-resolution PET-scanners used for pre-clinical imaging of small animals. This paper highlights the opportunity in using pre-clinical PET-imaging facilities in core analysis, and describes an ongoing collaboration that has successfully utilized this opportunity. Pre-clinical PET shares the advantages of clinical imaging in terms of radioisotope production, transportation and handling albeit with weight and size limitations not normally encountered using clinical scanners. A higher spatial resolution, however, results from the smaller size (due to decreased distance between scanned object and detector elements, and smaller detector element size, see e.g. Bailey *et al.* [1]), and the high-resolution PET-CT scanner used in this work features voxel sizes of 0.3-0.4 mm. Issues related to experimental duration may be largely overcome and the pre-clinical scanners available for longer continuous time spans, depending on the number and frequency of parallel animal studies.

Table 1 summarizes the obstacles associated with PET imaging in private facilities, and using existing clinical and pre-clinical imaging facilities. The table illustrates that several obstacles are overcome using pre-clinical PET imaging, but some remain; e.g. it may be a challenge using software and settings intended for soft-tissue small animals in studies on sedimentary rocks. Tailor-made software is an advantage reserved for geo-scientifically oriented, private PET-imaging facilities. Additionally, access requirements may vary between facilities; the pre-clinical PET-scanner used in this work is a part of the Molecular Imaging Centre (MIC) (Department of Biomedicine, University of Bergen, Norway) and is

Table 1 : General obstacles in PET-imaging may be overcome within medical imaging facilities- although new obstacles occur. An overview of obstacles for each option (private, clinical or pre-clinical PET-imaging) is shown below.

Obstacles	Present	Partly handled	Handled	
Production of radioisotopes	PET (general)		Pre-clinical PET	Clinical PET
Transportation of radioisotopes	PET (general)		Pre-clinical PET	Clinical PET
Safe handling of radioisotopes	PET (general)		Pre-clinical PET	Clinical PET
Experiment duration	Clinical PET	Pre-clinical PET		PET (general)
Access for personell	Clinical PET	Pre-clinical PET		PET (general)
IT access	Clinical PET	Pre-clinical PET		PET (general)
Software modification	Clinical PET	Pre-clinical PET		PET (general)
Cleanliness	Clinical PET	Pre-clinical PET		PET (general)
Spatial resolution	Clinical PET	PET (general)		Pre-clinical PET
Weight and size of laboratory equipment	Pre-clinical PET	Clinical PET		PET (general)

located at the PET-centre at Haukeland University Hospital.

MIC was started in 2003 and is an open access national (Normolim²) and international/European (Euro-BioImaging³) level, providing access to advanced small animal imaging to the research community. Obstacles related to researcher access have therefore been minor. MIC maintains instrumentation and has highly qualified scientific and technical personnel to facilitate a variety of research (usually in the field of biomedicine). Their experience in interacting across research groups have also made the leap from physiology to flow physics research relatively short. The existence of this operational open core facility is obviously a significant advantage in using pre-clinical PET-imaging for core analysis.

1.3 Availability of pre-clinical PET scanners

The pre-clinical PET-CT scanner used in this work is a nanoScan® PET-CT from Mediso, who is one of the main suppliers of pre-clinical PET scanners in addition to Bruker, MR Solutions and Siemens. Bruker reports 60-70 delivered pre-clinical PET scanners world-wide. Mediso reports 61 operational PET-CT and 30 PET-MRI scanners. MR Solutions do not wish to provide information about the exact number of scanners delivered by their company, but features more than ten customers on their web home page. Siemens no longer produce pre-clinical scanners, but some may still be in operation. Tracers used for animal studies are usually short-lived, and the PET-scanners are therefore often located in close proximity to cyclotrons.

1.4 Availability of cyclotrons

Medical cyclotrons are used to produce isotopes used in diagnostic imaging. More than 1200 cyclotrons exist world-wide, according to the International Atomic Energy Agency (IAEA) [27], and many are localized in close

proximity to research institutions and/or hospitals that are actively applying PET-imaging as a diagnostic tool.

A searchable and detailed overview of cyclotrons may be found at:

<https://nucleus.iaea.org/sites/accelerators/Pages/Cyclotron.aspx>, providing location, affiliation, make and model.

The cyclotron connected to the current research facility is shown in Fig. 2.



Fig. 2. World-wide map of cyclotrons from International Atomic Energy Agency (IAEA), with country and city inserts. Modified screenshot from [27].

2 Overcoming the obstacles

We have used the MIC pre-clinical PET-CT scanner since 2013 and have developed a procedure to routinely utilize shared pre-clinical imaging facilities for core analysis.

² Normolim: NORwegian MOLeclar IMaging infrastructure. More information available on normolim.w.uib.no

³ See eurobioimaging.eu for more information

Our experience is described, and attempted generalized, in the following; to highlight the possibilities of similar collaboration elsewhere.

2.1 Production of radioactive tracers

Medical imaging often utilizes short-lived radionuclides, produced at local cyclotrons. Radionuclides are attached to larger molecules before imaging. ¹⁸F (Fluorine-18) e.g. often substitutes the normal hydroxyl group in glucose to make radiotracer ¹⁸F-FDG (Fludeoxyglucose). The accelerated uptake of this glucose analogue by cancer cells enables visualization of cancerous tissue within the human body. ¹⁸F-FDG is also the most used radiotracer in fluid flow visualization for geoscientific purposes [21], due to its miscibility in water coupled with PET sensitivity. Minute amounts of ¹⁸F-FDG is needed to procure accurate, high-quality images, and can be added to water without notably altering its properties. E.g. in the MIC research facility the ¹⁸F-FDG concentration is high; at around 20 GBq in 24 mL of water directly after production. We typically receive <1 mL of this solution to label the desired aqueous solution. A variety of aqueous solutions have so far been labelled by ¹⁸F-FDG, including: brine, polymer solution and surfactant solution. The small volume of tracer compared to the aqueous solution volume ensures that macroscopic fluid properties are unaltered during PET imaging. This is one of the main advantages of PET-imaging compared to e.g. attenuation methods (exemplified by CT), where density contrasts are necessary to capture flow dynamics. ¹⁸F-FDG is routinely produced at the PET-centre (Haukeland University Hospital) to facilitate medical imaging, and trained personnel are available on a daily basis. Daily production of ¹⁸F-FDG for clinical use reduces the need for dedicated ¹⁸F-FDG production for pre-clinical imaging. The half-life of ¹⁸F-FDG is short, at $t_{1/2} = 109$ minutes, and it is delivered in vials as a liquid.

¹¹C (Carbon-11) can be attached to Carbon dioxide (CO₂) to make radiotracer ¹¹CO₂, suitable for explicit visualization of CO₂ flow in porous rocks. ¹¹CO₂ has a half-life of $t_{1/2} = 20$ minutes. The short half-life requires higher doses of radiation to be handled in flow experiments, because the radiation (which will, in turn, produce the PET signal) swiftly decays. The preferred state of radiotracer used for CO₂ flow experiments is gaseous- which also makes transfer more challenging (see Section 2.2).

The challenges related to production of radioisotopes are very well handled by trained personnel at the PET-centre. The end user- in this case core analysts aiming to use PET to visualize fluid flow- should therefore not perceive the production of radiotracers as a large obstacle. Basic understanding of radiation is, however, necessary to accurately design and implement flow experiments.

2.2 Safe transfer of radioactive tracers

Safe transportation of short-lived radiotracers varies with the type and state of radiotracer. This far in our work, ¹⁸F has been used as ¹⁸F-FDG mixed in water, delivered in vials within lead containers. The containers are taken into the imaging lab through a wall hatchway (Fig. 3). ¹⁸F-FDG radioactivity is measured and mixed with aqueous solution within the imaging lab. The obstacles related to transportation of liquid radiotracer at ambient conditions between labs in this facility are minor.

Transfer of gaseous ¹¹CO₂ is more challenging and requires an introduction to the layout of the interconnected labs (Fig. 3). ¹¹CO₂ is produced locally and transferred from the cyclotron through a hot cell (shielded nuclear radiation containment chamber) located at the chemistry lab. A Swagelok nylon tubing is connected to the hot cell in one end to prepare for gas transfer, stretched across the floor and through the wall hatchway to the control room. The other end of the tubing is connected to a receiving single-piston pump located within the PET-CT imaging lab. Two operators are needed for safe transfer: one operator present by the cyclotron, to transfer ¹¹CO₂ to the hot cell and monitor radiation levels within the receiving laboratories, and one operator monitoring and controlling the receiving pump. During gas transfer the radiation levels within both the chemistry and imaging lab are high, and both rooms should be empty. The receiving pump (Fig. 4) should therefore be remote controlled to avoid operator exposure to high levels of radiation.

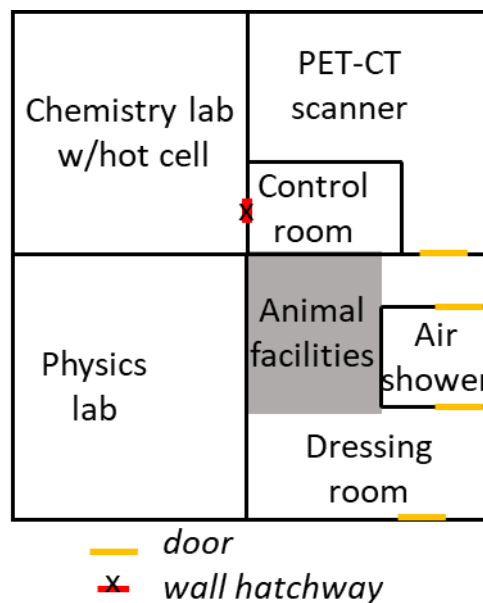


Fig. 3. Schematic layout of relevant labs at MIC/PET-centre.

¹¹CO₂ is sent to the hot cell by the cyclotron operator (normally a physicist or radiochemist employed at the PET-centre) and progresses directly through the tubing and into the pump, which should be empty and set to receive. Depending on CO₂ injection volume, rate, conditions and desired radiation dose, several consecutive

volumes of $^{11}\text{CO}_2$ may be transferred. The system is thereafter flushed by non-radioactive gas (N_2) to displace $^{11}\text{CO}_2$ from the tubing. When laboratory radiation levels have decreased sufficiently, the pump is isolated from the hot cell and connected to the experimental set-up (Fig. 4), by activating a set of valves. We use pressure- and remote-controlled valves for this purpose. Manual valves are also mounted on the pumps as a precaution. The received $^{11}\text{CO}_2$ is mixed and swiftly pressurized to the experimental conditions by transferring pre-pressurized CO_2 from a second pump (Fig. 4). Although obstacles remain and the risk for failure is higher when transferring gas (e.g. gas leakage could force temporary shut-down of several labs, with implications for hospital capacities), safe transfer has repeatedly been demonstrated, which enable visualization experiments of high scientific value (Section 3).

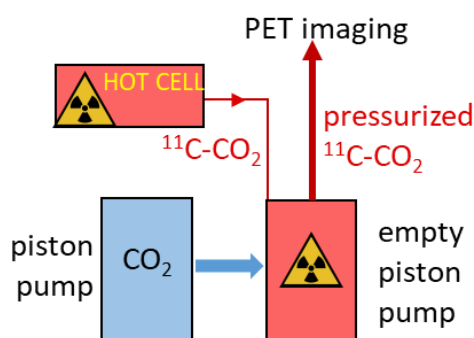


Fig. 4. Safe transfer of radioactive gas using two single-piston pumps. The pumps are connected to each other, the experimental setup and the hot cell via remote controlled valves.

2.3 Safe use and handling of radioactivity

During experimental work with radiotracers the well-known principles of radiation safety apply: ALARA, “as low as reasonably achievable”. The basic protective measures are to increase distance (from the radiation source), decrease time (close to the radiation source) and use proper shielding (between radiation source and personnel). Shielding is important both in terms of health, safety and environmental guidelines for workers (HSE) and to improve image quality, by avoiding radiation from the experimental setup into the PET scanner (increase in background radiation leads to higher level of noise in images). Portable lead walls have been used for shielding towards users in the control room and in adjacent imaging labs. During $^{11}\text{CO}_2$ injection radiation levels are initially high, and shielding walls have also been placed between the experimental setup and the PET-CT scanner, or the CO_2 pumps have been shielded by placing custom made lead rings around the pistons.

An additional important human safety precaution during core analysis with PET is to avoid leakages of radioactive fluids from the experimental setup. Hence; all parts of the setup, especially pumps, valves and line connections

should be checked thoroughly at the experimental conditions before radioactive fluids are introduced. Performing baseline tests with non-radioactive fluids is recommended. At ambient conditions, where radioactively labelled liquid is used at low radiation dose, manual control of pumps and effluent production is possible. $^{18}\text{F-FDG}$ mixed in aqueous solution may be produced into shielded graded cylinders, flasks or beakers where the radiation can decay, and is thereafter discharged according to local regulations. For more complicated experiments, for example injecting radioactive gas at high pressure conditions, installation of remote-controlled computers and pressure control valves is highly recommended. Hence; injection rates, direction of flow and fluid production may be monitored remotely and operator exposure to radiation minimized. Radioactive $^{11}\text{CO}_2$ should not be produced into air, and is collected in a piston accumulator at the production end of the core holder. The lower end of the accumulator is pressurized to the experimental conditions by mineral oil or distilled water, which is produced through a back-pressure regulator as produced effluents accumulate above the piston. After decay, the gas is vented into air. Image acquisitions may be remote controlled from an office outside the preparation room. The PET signal is typically recorded in time spans of 20 min – 2 hours per acquisition, and the signal is post-processed into three-dimensional images. The temporal resolution in each image frame is flexible and set during post-processing.

2.4 Weight and size of laboratory equipment

Safe transfer and use of radioactively labelled fluids for PET imaging is only possible by choosing suitable experimental equipment. Experimental conditions, such as pressure and temperature, and possibilities, such as flow rates and directions, directly relates to the different mechanical parts of an experimental setup, and their inherent limitations. Inevitably: operational limits of equipment often relate to their weight and size.

Clinical scanners are intended for human use, hence the gantry opening diameter is larger and can fit large and heavy equipment. Because the PET detector elements are also larger and positioned further away from the imaged object, the spatial resolution will, however, decrease. High-resolution (pre-clinical) PET scanners tend to have smaller gantry openings, which improves spatial resolution but also limits the possible size of an imaged object. In our case, the size of equipment that can be moved into the PET-scanner (i.e. core and core holder) is limited by 1) the gantry opening diameter (16 cm), 2) the PET field of view (FOV) of $120 \times 120 \times 97\text{mm}$ in the x,y,z directions, and 3) a mechanical arm which moves the equipment into the FOV and has inherent weight limitations (Fig. 5).

Several experiments have been performed using epoxy-coated cores, where the core circumference is cast in epoxy and the end faces are fitted with POM (polyoxymethylene) end pieces that are attached to nylon

fittings and lines [28-33]. The most influential factors in terms of weight are then the core material and saturating fluids. Use of epoxy allows flexibility in terms of core shape and defined no-flow boundaries, and small cores may be aligned either horizontally or vertically within the

albeit with consequences for the total weight of the equipment.

The mechanical arm moves the core horizontally for positioning within the CT and PET FOV. The core is

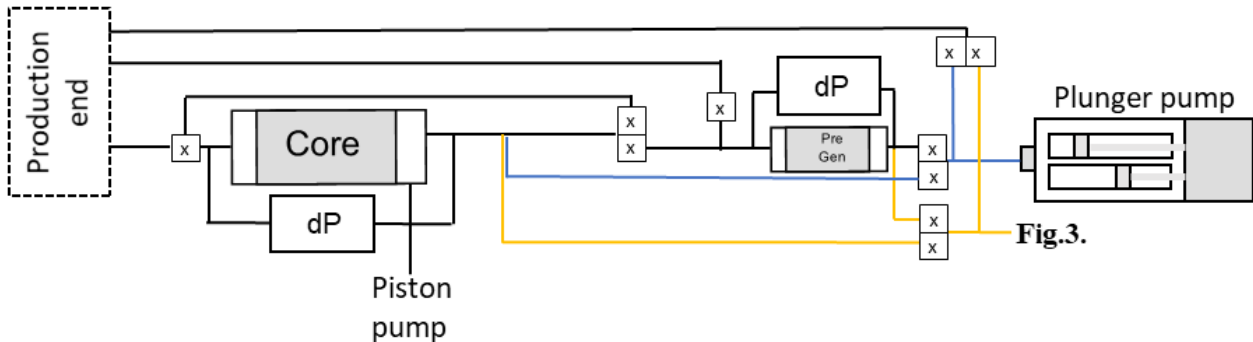


Fig. 6. Example of experimental setup used for PET imaging of CO₂-foam. The setup is very flexible, and can with few adjustments be used for a variety of experiments. «x» marks pressure-control valves and «dP» marks pressure measurements. CO₂ only flows in orange lines and only the aqueous phase in blue lines. The production end varies with radioactively labelled phase, as described in Section 2.3.

scanner. Experimental investigations of subsurface carbon sequestration, however, often require relevant conditions, i.e. higher pressures, and it is necessary to use a core holder and apply overburden pressure to the core.



Fig. 5. A custom-made core holder by RS systems © (Trondheim, Norway) is installed on a mechanical arm for imaging with high-resolution PET.

The core holder is then the single most influential factor in terms of weight, and the pressurizing fluid, fittings, valves, lines, core and saturating fluid will also contribute to the total weight. We use a custom-made, aluminium core holder (Fig. 5) for our setup (©RS systems, Trondheim, Norway). The core holder is attached directly to the mechanical arm, and can fit cores of 1.5'' diameter and 10cm length. The core holder can withstand confinement pressure up to 200Bar. With thicker aluminium walls, higher pressures may be achieved-

always horizontally aligned when using the core holder. Epoxy coated cores rest on plastic animal beds attached to the mechanical arm and can also be oriented at an angle. In the combined Mediso PET-CT, the CT scanner is located further into the scanner, and the PET scanner ring is located closer to the gantry opening. The two modalities are run in sequence and simultaneous images from the two modalities cannot be acquired. The mechanical arm moves the core between modalities and is controlled by the operator through the scanner software. CT is initially acquired to position the core. The mechanical arm thereafter moves the core into the defined position for PET acquisition. Lines connecting the core holder to the experimental setup therefore needs to be flexible and allow for horizontal movement during experiments. We have successfully used both 1/8'' peek and 1/16'' stainless steel lines, due to their low weight, flexibility and ability to withstand high pressures.

Another obstacle in terms of size and weight during pre-clinical imaging is that all equipment must pass through the air shower illustrated in Fig. 3. The purpose of the air shower is to remove animal allergens from researchers going out of the imaging lab. Air showers are proven effective to remove allergens from hair and clothes, to prevent spreading to the surrounding facilities. Because the imaging lab and surrounding facilities were intended for animal studies and users, this procedure must be followed also during core analysis (it is not possible to physically bypass the air shower). We have solved this for our use by mounting all laboratory equipment (pumps, accumulators, core holder, pressure transducers etc) on a portable trolley, that fits within the air shower (width 60cm, length 100cm). The trolley is wheeled into the imaging lab through the air shower before imaging experiments, and is stored in the physics lab (Fig. 3) in between experiments. In lab facilities shared by several research disciplines, compact and easily transportable

experimental setups are necessary, as the time available for imaging may be short (down to few days).

3 Opportunities in CCUS

Permanent storage of CO₂ in deep sedimentary reservoirs is being developed worldwide, to curb atmospheric carbon emissions. Demonstrations of safe storage on the field scale must be supported by experimental data on smaller scales, to fully understand how CO₂ storage influences, and is influenced by, the pore space. PET imaging has significant potential to capture dynamics during CO₂-flow in porous media, both implicitly (labelling the aqueous phase) and explicitly (radioactively labelling the CO₂). This section summarizes the opportunities and demonstrated potential for PET in CCUS (Carbon Capture Utilization and Storage) research. For an overview of previous application of PET imaging in water resources research, we refer to Zahasky *et al.* [21].

An example experimental setup is demonstrated in Fig. 6: the setup is designed to be flexible and can easily be modified for the purpose of the experiment, e.g. to facilitate circulation of fluids at the inlet end face.

3.1 CO₂ storage

In-situ experimental observations of forced CO₂ displacement into porous media is necessary to explain the influence of heterogeneities on CO₂ saturation development and capillary trapping: to accurately predict CO₂-brine migration in carbon sequestration reservoirs. Fernø *et al.* [2] initially demonstrated decoupled PET-CT imaging for CO₂ storage applications. They injected CO₂ into water-saturated sandstone at 90 Bar pressure to measure decoupled saturation information from each method. CO₂ saturation development was determined implicitly by quantifying the decrease in signal from ²²Na-labelled (half-life of 2.6 years) water, using a clinical PET-CT scanner with lower spatial resolution. Exhaustive sensitivity studies comparing PET and CT imaging were performed by Pini *et al.* [7] and Zahasky and Benson [3], applying a previously derived analytical method [6, 34] to extract capillary pressure and relative permeability functions on the sub-core scale. Zahasky and Benson [3] used high-resolution PET imaging to measure single- and multiphase transport properties in heterogeneous sandstone during gas injections: Nitrogen constituted the gas phase and the pressure was approximately 1.4 Bar, i.e. the experimental conditions were less relevant for CCUS, but the data analysis provided a solid foundation for using

PET in further quantification experiments. Zahasky and Benson [35], [36] also used high-resolution PET to investigate CO₂-flow and trapping in heterogeneous sandstone cores at pressures ranging from 1-8 Bar. CO₂ displacement was implicitly imaged by injecting pulses of ¹⁸F-FDG labelled water, or co-injecting water and Nitrogen. PET-imaging was again repeatedly and successfully used to assess flow parameters on the sub-core scale. Brattekkås and Haugen [37] recently demonstrated explicit and dynamic imaging of CO₂ during flow through a low-permeable chalk core at elevated pressure conditions. High-resolution PET imaging was used to visualize CO₂, labelled explicitly by ¹¹C-CO₂ and injected into a chalk core at 50 Bar pressure (Fig. 7). The procedure for CO₂ radiolabelling and injection was similar to the procedure detailed in Section 2; and accurate quantification of spatial phase saturations were achieved during both brine and CO₂ injections, at the [mm] scale. Visualization revealed heterogeneous displacement patterns, as expected during gas-brine displacements at less-than-ideal mobility ratio. The heterogeneities were attributed to a sub-core variation in permeability, which could be determined from PET displacement data at the millimetre scale.

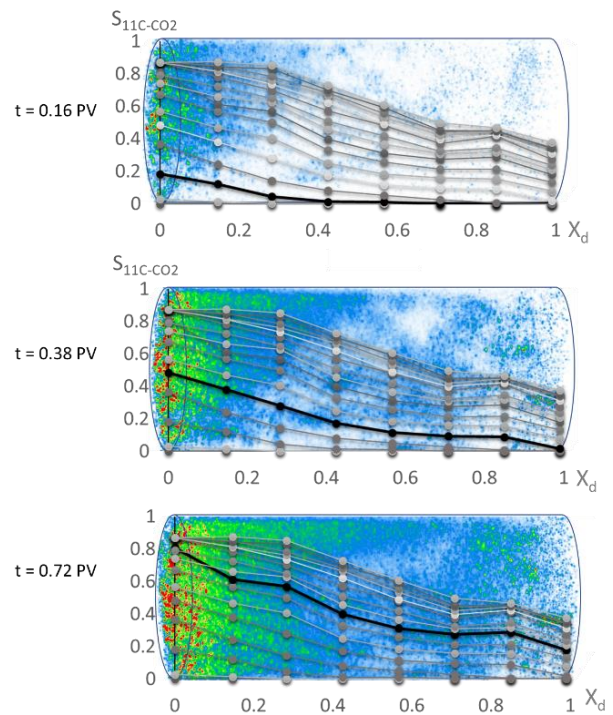


Fig. 7.⁴ Dynamic saturation development during ¹¹C-CO₂ injection into a chalk core, demonstrated by three timesteps. Qualitative 3D images of core saturation are overlaid by quantitative 1D profiles derived from PET. The red colour in 3D images represents the highest PET signal intensity, followed by green and blue. White areas do not contain ¹¹C-CO₂. The variations in the colour map hence indicate large spatial

⁴ A modified version of this figure was first published in *Explicit tracking of CO₂-flow at the core scale using Micro-*

variations in CO₂ saturation. The experiment and results are detailed in [37].

These recent publications illustrate that PET imaging can (and should) be utilized to investigate CO₂-brine displacements at a range of conditions and flow rates, where insight into local saturations and flow patterns allow for accurate determination of flow functions. Few publications are yet available where CO₂ injection is captured with high-resolution PET at high pressure conditions; but may be provided as necessary by broader access to PET imaging technology.

Spontaneous imbibition is another important mechanism during CO₂ sequestration, and may control the redistribution and remobilization of fluids after CO₂ injection. High-resolution PET imaging has in several instances been used to image the imbibing, radioactively labelled, water front [28-30]. The results confirmed that PET is an excellent tool to quantify dynamics during spontaneous imbibition, **Fig. 8**.

Fig. 8. PET imaging was previously used to confirm piston-like behaviour during spontaneous imbibition [28], and to visualize and explain behaviour deviating from general assumptions [33].

PET imaging can confirm the assumption of piston-like behaviour necessary to extract relative permeability and capillary pressure from spontaneous imbibition data [28], or provide insight to displacement patterns deviating from the general assumptions, where extraction of flow functions would be inaccurate [33]. The referenced works were simple in terms of experimental conditions and equipment: using epoxy-coated cores at ambient conditions. With minor adjustments, however, the high-pressure experimental setup in **Fig. 6**. can be modified for high-pressure spontaneous imbibition at relevant CO₂ storage conditions, applying e.g. the method proposed in Zahasky and Benson [38]. Relevant saturation functions for CCUS can then be extracted from the data set when important assumptions are confirmed by imaging.

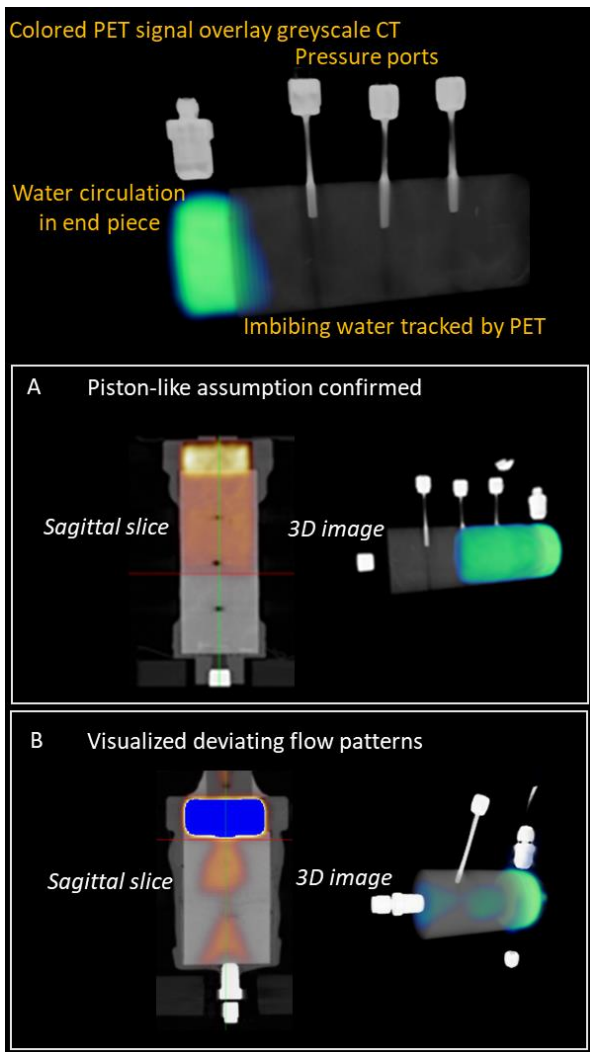
3.2 CO₂ utilization (CO₂-EOR)

Combined CO₂ storage and enhanced oil recovery (EOR) can lower the carbon footprint of produced oil, while improving the recovery factor in many reservoirs. PET imaging can provide insight into complex flow systems used for EOR applications; including the flow of complex fluids such as polymers [39], polymer gels [32, 40-42] and foams [10] in heterogeneous and fractured porous media.

Displacement of oil by CO₂ can be imaged by PET similarly to CO₂-brine displacements (**Section 3.1**) using ¹¹C to explicitly label CO₂. Water and CO₂ flow may be explicitly imaged by PET in the same pore network, but each fluid must then be allowed to decay before injection of the other- i.e. only one fluid phase may be imaged at a time. Multimodal imaging by PET-CT [2] or PET-MRI [26] allows for explicit and simultaneous imaging of up to three fluid phases within the same porous medium, with high potential benefits for core scale research.

Foam represents an opportunity to reduce CO₂ mobility, to improve the displacement of oil. Foam is a dispersion of gas separated by liquid lamella, where both foam constituents may often be imaged by PET: aqueous surfactant solution labelled by ¹⁸F-FDG or injected CO₂-foam gas phase labelled by ¹¹CO₂. Brattekkås *et al.* [10] used PET imaging to quantify foam flow in natural fracture networks, where an impermeable matrix ensured fluid flow in the fracture network only. The spatial resolution of PET is too low to facilitate direct observation of foam structure (bubble size etc), but is an efficient tool to establish foam distribution within fractures. PET may also be used to establish improved sweep efficiency within adjacent (permeable) matrix.

Polymer gel is often used for water shutoff purposes, and may also have significant potential in CO₂-EOR applications. Polymer gel reduce fracture conductivity,



without influencing matrix properties; hence, polymer gel placed in fractures improve sweep efficiency by diverting subsequently injected fluids into the matrix. Previous studies showed that the efficiency of polymer gel in EOR is heavily dependent on core wettability, the properties of the fracture-filling gel, and the properties of the chase fluid [43]. CO₂ has several inherent benefits as a chase fluid, such as miscibility with matrix oil. Recent studies demonstrated that PET imaging is an efficient method to establish gel behaviour and matrix sweep during chase floods. Brattekkås *et al.* [32] used PET imaging and ¹⁸F-FDG labelled water to gain insight into dynamics during chase waterflooding of gel-filled fractures. The water injection rate was initially low, and gel rupture was controllably measured: the pattern of gel rupture was found to be heterogeneous within the fracture, and its width could not be derived from global measurements of flow rate and differential pressure. Further, Brattekkås and Seright [31] and Brattekkås and Seright [42] used PET imaging to establish how the rupture channels through gel evolved when the salinity of the injected water-phase was reduced. They proved that gel swelled when contacted by low-salinity water and consequently improved fracture blocking efficiency. The coupled dynamics of gel-swelling with continuous water injection improved matrix displacement in fractured cores. The studies used ¹⁸F-FDG mixed in high-salinity or low-salinity water to explicitly image water flow through the gel-filled fractures and adjacent matrix. The gel was first ruptured using high-salinity water (w/¹⁸F-FDG), which was flushed out or decayed before low-salinity water w/¹⁸F-FDG was imaged. Because of the short half-life of ¹⁸F-FDG, tracing of several water composition was possible within the duration of the experiments; i.e. hours to days. PET imaging was a significant advantage in assessing the behaviour of different water phases within gel-filled fractures: where other imaging methods would require chemical alterations of the water phase(s) or gel (e.g. using D₂O instead of H₂O for MR imaging, or adding sodium iodide for CT imaging) to distinguish the behaviour of the injected phase from gel or previously injected water. The PET signal is not influenced by injected fluids that have decayed, hence the labelled phase is tracked during injection without disturbances from the surroundings.

3.3 CO₂ storage security

PET imaging has significant potential in establishing seal security for CO₂ storage applications. Seal ability to prevent leakage of buoyant CO₂ is important in field scale applications; and demonstration of safe CO₂ storage is crucial to implement widespread CCUS. Fernø *et al.* [25] used a clinical PET-CT scanner to visualize CO₂ flow in tight shale and demonstrated the excellent sensitivity of PET imaging compared to CT in tight, low-porous and -permeable rocks, **Fig. 9**; where a very low volume of ¹¹C-

CO₂ was sufficient for PET quantification of saturation. The uneven fluid displacement within shale, visible by PET, could be tied to structural heterogeneities, visible by CT.

PET imaging could be further used to quantify CO₂ capillary entry pressure in seals by modifying established methods (previously summarized in e.g.

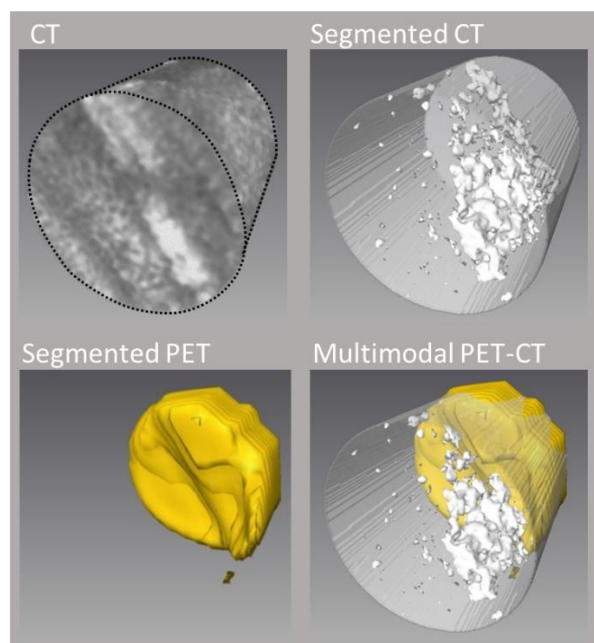


Fig. 9⁵. PET imaging captures the inflow of ¹¹C-¹⁸O₂ in tight shale. The nonuniform displacement front can be tied to structure, visible by CT. For in-depth discussion and results of the experiment showed in the figure we refer to [25].

[44]) for imaging. The established experimental methods (without imaging) applies pressure to CO₂ in contact with the core end face, either stepwise (step-by-step approach) or continuously (continuous injection approach), while pressure and production is monitored and logged. The capillary entry pressure may be calculated from pressure and production data when the cores are assumed to be homogeneous. The same approach may be followed during imaging, applying ¹¹C-¹⁸O₂ pressure at the inlet end face of the core (**Fig. 6**) and monitoring gas entry into the core by PET, and the capillary entry pressure may be extracted by connecting the imaged gas entry to pressure data. The high temporal resolution of PET ensures that the entry pressure is measured at the correct time, and the influence of core heterogeneities is accounted for rather than neglected. Longer-term experiments to assess seal wettability or CO₂ diffusion, which are also important in terms of seal security [45], are more challenging and requires radiotracers with longer half-lives to be assessed by PET.

⁵ A modified version of this figure was first published in *Description of CO₂ EOR and Storage in Tight Shale*

CO₂ storage is most commonly developed in sandstone formations, but carbonates also play an important role in the development and widespread implementation of CCUS: both due to the world-wide abundance of saline aquifers within carbonate formations, and as candidates for CO₂-EOR with combined storage. Acidification of formation brine during CO₂ injection in carbonates may cause dissolution of the rock material and reactive flow patterns are developed that significantly influence fluid flow and, inevitably, carbonate CO₂ storage security. PET imaging enables experimental investigations of reactive transport dynamics at the core scale. Dynamic quantification of dissolution (rate and degree) at the core scale may further support upscaling to larger scales. **Fig. 10** shows preliminary images from an ongoing dissolution study. The CT modality shows structural changes in the core resulting from dissolution. The PET modality shows changes in the preferred fluid flow pattern, consistent with the development of wormholes. Carbonate dissolution and formation of wormholes was previously observed using CT [46, 47]. Multi-modal PET-CT imaging represents a new addition to the experimental portfolio available to study dissolution; by simultaneously connecting the flow of labelled fluids to the structure through which it flows, **Fig. 10**. The unique contribution of PET imaging to dissolution studies is, hence, to non-invasively, dynamically and explicitly study the development of fluid flow patterns. Flow patterns may be tied to minor or major changes in structure by CT scans. CT scans may be performed either dynamic, pre- and/or post- flow experiment imaging. Pre- and post-imaging of micro-CT may than also be applied to visualize structural changes at a much higher spatial resolution.

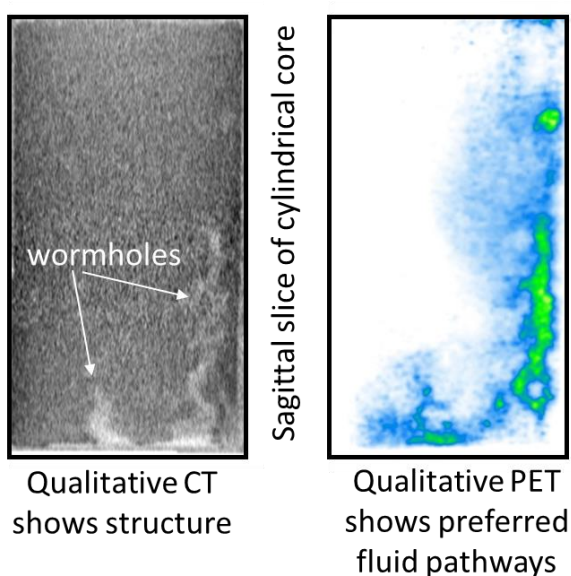


Fig. 10: Dissolution of carbonate during CO₂ or carbonated water injection is often visualized using CT, but PET imaging may be an important contribution. While CT (left) portrays structural changes during dissolution, PET determine dynamic changes in the preferred flow paths within the core.

This work was supported by Norwegian Research Council under project 280341. The authors acknowledge Kristine Fasmer and Kjartan Foldnes for valuable help during radiotracer production and transfer, and PET-imaging. Thank you to Torunn Veien and Olav Parelius Folkvord (UiB MSc students) for providing image data from ongoing dissolution studies. Pre-clinical imaging is routinely performed at the Molecular Imaging Center, Dept. of Biomedicine, University of Bergen. Personnel and equipment associated with the PET-centre at Haukeland University Hospital contributes greatly to the collaboration. The mechanical workshop at the Dept. of Physics and Technology, University of Bergen tailored experimental equipment to our needs, for which the authors are thankful.

References

1. Bailey, D.L., et al., eds. *Positron Emission Tomography*. Basic Sciences. 2005, Springer.
2. Fernø, M.A., et al., *Combined positron emission tomography and computed tomography to visualize and quantify fluid flow in sedimentary rocks*. Water Resources Research, 2015.
3. Zahasky, C. and S.M. Benson, *Micro-positron emission tomography for measuring sub-core scale single and multiphase transport parameters in porous media*. Advances in Water Resources, 2018. **115**: p. 1-16.
4. Krevor, S.C.M., et al., *Capillary heterogeneity trapping of CO₂ in a sandstone rock at reservoir conditions*. Geophysical Research Letters, 2011. **38**(15): p. L15401.
5. Krevor, S.C.M., et al., *Relative permeability and trapping of CO₂ and water in sandstone rocks at reservoir conditions*. Water Resources Research, 2012. **48**(2): p. W02532.
6. Pini, R., S.C.M. Krevor, and S.M. Benson, *Capillary pressure and heterogeneity for the CO₂/water system in sandstone rocks at reservoir conditions*. Advances in Water Resources, 2012. **38**(0): p. 48-59.
7. Pini, R., et al., *Quantifying solute spreading and mixing in reservoir rocks using 3-D PET imaging*. J. Fluid Mech., 2016. **796**: p. 558-589.
8. Brattekkås, B., et al., *New Insight to Wormhole Formation in Polymer Gel during Water Chases*. *Proceedings of the SPE Bergen One Day Seminar*. 2016: Bergen, Norway.
9. Dechsiri, C., et al., *Positron emission tomography applied to fluidization engineering*. Can J Chem Eng, 2005. **83**(1): p. 88-96.
10. Brattekkås, B., et al., *Foam Flow and Mobility Control in Natural Fracture Networks*. Transport in Porous Media, 2020. **131**(1): p. 157-174.
11. Khalili, A., A.J. Basu, and U. Pietrzyk, *Flow visualization in porous media via Positron Emission Tomography*. Phys Fluids, 1998. **10**(4): p. 1031-1033.
12. Kulenkampff, J., et al., *Evaluation of positron-emission-tomography for visualization of migration processes in geomaterials*. Phys Chem Earth, 2008. **33**((14-16)): p. 937-942.
13. Maucec, M., et al., *Imaging of Fluid Mobility in Fractured Cores Using Time-lapse Positron Emission Tomography*, in *SPE Annual Technical Conference and Exhibition*. 2013, Society of Petroleum Engineers: New Orleans, LA, USA.

14. Maguire, R.P., et al., *Positron emission tomography of large rock samples using a multiring PET instrument*. Ieee T Nucl Sci, 1997. **44**(1): p. 26-30.
15. Degueldre, C., et al., *Porosity and pathway determination in crystalline rock by positron emission tomography and neutron radiography*. Earth Planet Sc Lett, 1996. **140**((1-4)): p. 213-225.
16. Emery, G.T., *Perturbation of Nuclear Decay Rates*. Annual Review of Nuclear Science, 1972. **22**(1): p. 165-202.
17. Haugan, A. *A Low-Cost PET System for Use in Flow Experiments of Porous Media*. in *SPE Annual Technical Conference and Exhibition*. 2000. Dallas, Texas.
18. Kulenkampff, J., et al., *Evaluation of positron-emission-tomography for visualisation of migration processes in geomaterials*. Physics and Chemistry of the Earth, 2008. **33**(14-16): p. 937-942.
19. Richter, M., et al., *Positron emission tomography for modelling of geochemical transport processes in clay*. Radiochimica Acta, 2005. **93**: p. 643-651.
20. Gründig, M., et al., *Tomographic radiotracer studies of the spatial distribution of heterogeneous geochemical transport processes*. Applied Geochemistry, 2007. **11**: p. 2334-2343.
21. Zahasky, C., et al., *Positron emission tomography in water resources and subsurface energy resources engineering research*. Advances in Water Resources, 2019. **127**(May 2019): p. 39-52.
22. Rohren, E.M., T.G. Turkington, and R.E. Coleman, *Clinical Applications of PET in Oncology*. Radiology, 2004. **231**(2): p. 305-332.
23. Anand, S.S., H. Singh, and A.K. Dash, *Clinical Applications of PET and PET-CT*. Medical journal, Armed Forces India, 2009. **65**(4): p. 353-358.
24. Bailey, D.L., et al., *Positron Emission Tomography*, ed. M.N. Maisley. 2005: Springer.
25. Fernø, M.A., et al., *Flow visualization of CO₂ in tight shale formations at reservoir conditions*. Geophysical Research Letters, 2015. **42**: p. 7414-7419.
26. Brattekkås, B., et al., *Unlocking multimodal PET-MR synergies for geoscience*. Advances in Water Resources, 2020. **142**: p. 103641.
27. Agency, T.I.A.E. <https://nucleus.iaea.org/sites/accelerators/Pages/Cyclotron.aspx>. 2020.
28. Fernø, M.A., et al., *Quick and Affordable SCAL: Spontaneous Core Analysis*, in *The International Symposium of the Society of Core Analysts*. 2015: St.John's, Newfoundland&Labrador, Canada.
29. Fernø, M.A., et al., *Spontaneous Imbibition Revisited: A New Method to Determine Relative Permeability and Capillary Pressure by Inclusion of the Capillary Backpressure*, in *EAGE 18th European Symposium on Improved Oil Recovery*. 2015: Dresden, Germany.
30. Ruth, D., et al. *Matching Experimental Saturation Profiles by Numerical Simulation of Combined Co-/Counter-Current Spontaneous Imbibition*. in *International Symposium of the Society of Core Analysts*. 2016. Snowmass, CO, USA.
31. Brattekkås, B. and R.S. Seright, *Implications for improved polymer gel conformance control during low-salinity chase-floods in fractured carbonates*. Journal of Petroleum Science and Engineering, 2018. **163**: p. 661-670.
32. Brattekkås, B., et al., *New Insight Into Wormhole Formation in Polymer Gel During Water Chase Floods With Positron Emission Tomography*. SPE Journal, 2017. **22**(01): p. 32-40.
33. Føyen, T.L., M.A. Fernø, and B. Brattekkås, *The Effects of Nonuniform Wettability and Heterogeneity on Induction Time and Onset of Spontaneous Imbibition*. SPE Journal, 2019. **24**(03): p. 1192-1200.
34. Pini, R. and S.M. Benson, *Simultaneous determination of capillary pressure and relative permeability curves from core-flooding experiments with various fluid pairs*. Water resources research, 2013. **49**(6): p. 3516-3530.
35. Zahasky, C. and S.M. Benson. *Phase saturation validation and tracer transport quantification using microPET in a heterogeneous sandstone core*. in *International Symposium of the Society of Core Analysts*. 2016. Snow Mass, Colorado, USA: Society of Core Analysts.
36. Zahasky, C. and S.M. Benson, *Using micro-positron emission tomography to quantify single and multiphase flow in heterogeneous reservoirs*. Energy Procedia, 2017. **114**: p. 5070-5082.
37. Brattekkås, B. and M. Haugen, *Explicit tracking of CO₂-flow at the core scale using micro-Positron Emission Tomography*. Journal of Natural Gas Science and Engineering, 2020. **77**.
38. Zahasky, C. and S.M. Benson, *Spatial and temporal quantification of spontaneous imbibition*. Geophysical Research Letters, 2019.
39. Sandnes, M.F., *Wetting Stability of Aged Limestone in the Presence of HPAM Polymer*, in *Department of Physics and Technology*. 2020, University of Bergen: Bergen Open Research Archive.
40. Brattekkås, B. and M.A. Fernø, *New Insight from Visualization of Mobility Control for Enhanced Oil Recovery Using Polymer Gels and Foams*, in *Chemical Enhanced Oil Recovery (cEOR) - a Practical Overview*, L. Romero-Zèron, Editor. 2016, InTech.
41. Brattekkås, B. and R.S. Seright, *Implications for improved polymer gel conformance control during low-salinity chase-floods in fractured carbonates*. Journal of Petroleum Science and Engineering, 2017.
42. Brattekkås, B. and R. Seright, *The Mechanism for Improved Polymer Gel Blocking During Low-Salinity Waterfloods, Investigated Using Positron Emission Tomography Imaging*. Transport in Porous Media, 2020. **133**(1): p. 119-138.
43. Brattekkås, B., et al., *Fracture Mobility Control by Polymer Gel- Integrated EOR in Fractured, Oil-Wet Carbonate Rocks*, in *EAGE Annual Conference & Exhibition incorporating SPE Europec*. 2013: London, UK.
44. Busch, A. and N. Müller, *Determining CO₂ /brine relative permeability and capillary threshold pressures for reservoir rocks and caprocks: Recommendations for development of standard laboratory protocols*. Energy Procedia, 2011. **4**: p. 6053-6060.
45. Iglauer, S., C.H. Pentland, and A. Busch, *CO₂ wettability of seal and reservoir rocks and the implications for carbon geo-sequestration*. Water Resources Research, 2015. **51**(1): p. 729-774.
46. Menke, H.P., et al., *Dynamic Three-Dimensional Pore-Scale Imaging of Reaction in a Carbonate at Reservoir conditions*. Environmental science & technology, 2015. **49**: p. 4407-4414.

47. Ott, H., et al., *Core-flood experiment for transport of reactive fluids in rocks*. Review of Scientific Instruments, 2012. **83**(8): p. 084501.

